Available online at www.sciencedirect.com
SCIENCE DIRECT®
Journal of Electrostatics 64 (2006) 263–272
Journal of ELECTROSTATICS
www.elsevier.com/locate/elstat

A new method for generation of synchronised capacitive sparks of low energy

Erlend Randeberg*, Werner Olsen, Rolf K. Eckhoff

Department of Physics and Technology, University of Bergen, Allégaten 55, N-5007 Bergen, Norway

Received 15 March 2005; received in revised form 6 June 2005; accepted 7 July 2005
Available online 8 August 2005

Abstract

Conventional tests for investigating the minimum ignition energy (MIE) of dust clouds are restricted to energies above a few mJ, due to the challenges of producing sparks of very low energies that can be synchronised with a transient dust cloud. In this paper, a new circuit for generating capacitive sparks of significantly lower energies than 1 mJ is presented. A measurement system for capturing voltage and current waveforms has been integrated in the circuit, offering the energy delivered to the spark by integration of the power-versus-time curve. When working with such low energy discharges, which are highly transient phenomena, attention must be paid to the measurement technique and methods of noise reduction in the measurement instruments.

The measured spark energies range from 0.03 to 7 mJ, and they were found to constitute between 60 and 90 per cent of the energy stored on the discharge capacitors prior to breakdown. Losses to the measurement resistors are increasingly significant at higher energies and larger electrode gaps, due to the relatively large currents, and correspondingly small spark resistances.

A simple circuit simulation, in which the spark conductivity is assumed proportional to the spark energy, offers voltage and current waveforms in good agreement with the measured ones, indicating that the spark is mainly resistive. In addition, the discharge channel's ability to carry current depends strongly on the supplied energy. The proportionality factor is found to depend on the breakdown voltage.

Keywords: Spark generation; Spark energy measurement; Minimum ignition energy; Dust explosion

1. Introduction

When assessing the risk involved in handling combustible dusts or gases, the ignitability by electric sparks is central. The minimum ignition energy (MIE) is an important parameter, indicating the lowest energy capable of causing ignition. Current standard tests for evaluation of MIE for dust clouds, however, are limited to investigation of sparks of energies above a few mJ [1,2].

Several gases have MIEs significantly below 1 mJ, reported e.g. by Lewis and von Elbe [3]. However, a fundamental difference between experimental gas mixtures and dust clouds is the inevitable dynamics of dust clouds. A quiescent dust cloud is impossible because of gravitational particle settling. In the case of transient dust clouds the spark ignition source must be triggered at a point in time when the dust concentration is within its explosive limits. Therefore, precise synchronisation between generation of a transient dust cloud (dust dispersion) and sparking is essential when investigating the MIEs of such dust clouds. The synchronisation represents a challenge when working with low-energy capacitive sparks. For example, switches may add stray capacitance to the circuit, and thus add additional energy to the spark.

Routine testing of a wide range of dusts has revealed that many dusts ignite at energies lower than current standard apparatus can produce, i.e. a few mJ, and in

*Corresponding author. Tel.: +47 55589407; fax: +47 55589440.
E-mail address: erlend.randeberg@ift.uib.no (E. Randeberg).

0304-3886/$ - see front matter © 2005 Elsevier B.V. All rights reserved.
doi:10.1016/j.elstat.2005.07.001

such cases the true MIE remains unknown. However, using equipment different from the standard apparatus, Bartknecht [4] reported an MIE value for aluminium of 0.1 mJ and for sulphur of 0.01 mJ. But no details of the apparatus used were given.

When assessing the electrostatic ignition hazard of dust clouds in the range below 1 mJ, there is therefore a need for a test method that can yield practical relevant sparks, i.e. simple pure capacitive discharges of low energies. Furthermore, precise spark energy measurements in the low-energy region are useful to enable establishment of accurate MIE values, and can give valuable information on spark voltage and current waveforms.

The present paper describes a simple ignition system that can generate purely capacitive discharges of low energy, with an integrated spark energy measurement system for evaluation of the spark energy.

2. Generation of sparks and measurement of spark energies

2.1. Current spark generation principles

A number of circuits have been used for generating electric sparks for gas and dust ignition. When the spark is used as an ignition source for dust clouds, the need for a synchronisation between dust dispersion and sparking is evident.

The methods previously reported for dust cloud ignition can be separated into the following categories (unless otherwise stated, reference is made to [1]):

1. *Spark triggering by the use of a high-voltage relay*: For low energies, the unavoidable stray capacitance of the electrode arrangement is of the same order of magnitude as the storage capacitor, i.e. some pF, and must be taken into account when calculating the energy stored in the circuit prior to discharge. Very low energies are thus difficult to achieve with this arrangement.
2. *Spark triggering by voltage increase, using a high-voltage switch for slow charging of a capacitor through a large resistor*: The voltage at the time of breakdown is measured by an electrostatic voltmeter, which may introduce a certain stray capacitance. Precise synchronisation of the spark and dust dispersion can be difficult to achieve due to the charging time of the capacitor before discharge. Continuous charging of the storage capacitor may also cause a problem of multiple sparks within the time frame of the dust dispersion, especially at low capacitances when the time constant RC is small. To be able to generate single sparks of low energies, impractically high resistor values ($\sim 10^{11}\,\Omega$) must be used.
3. *Spark triggering by electrode movement*: The storage capacitor is charged to a high-voltage with the electrode gap so wide that breakdown is beyond reach. After opening of a charging relay, the grounded electrode is moved rapidly by a pneumatic or spring-driven system. Sparkover occurs at an unknown gap distance, corresponding to the field strength at breakdown. Corona current flowing from the electrode tips prior to breakdown may constitute a significant part of the stored energy at low energies, and the method is thus not ideal for low energies.
4. *Spark triggering by an auxiliary spark achieved using a three-electrode system*: A storage capacitor is charged to a high-voltage somewhat below breakdown. After closing a charging relay between capacitor and spark gap, an auxiliary spark of low energy is triggered, causing breakdown between the main electrodes. Corona current may cause energy losses, which can be significant at low energies. In addition, at low energies, the energy supplied by the auxiliary spark may be substantial compared to the stored capacitor energy in the primary circuit.
5. *Spark triggering by the use of a high-voltage transformer*: A triggering capacitor charged at a low voltage is discharged through a high-voltage transformer, generating an auxiliary high-voltage pulse. After breakdown, the main capacitor, initially charged to a voltage in the range of 500 V, is discharged in the spark gap. A diode is added across the main capacitor to prevent oscillations during discharge, thus attaining discharge characteristics similar to those of an over damped RC discharge. The lower limit of the spark energy that can be produced by this circuit is the energy of the triggering capacitor prior to breakdown, which has to be at least a few mJ.
6. *Spark triggering by irradiation of the electrode gap*: This method is similar to the three-electrode system (4), using highly energetic radiation to ionise the electrode gap instead of an auxiliary spark, and the limitations are the same. The opaqueness of dust clouds also causes problems.
7. *Spark triggering methods involving complex high-voltage circuit elements such as thyratrons*: Pulse forming networks may be used to generate sparks of specified duration and voltage [5–8]. Very low energies have been achieved using this kind of high-voltage equipment. However, working with such equipment offers significant technical challenges, and the sparks obtained may be quite "exotic" compared to the sparks occurring in industrial practice.

All the spark generation principles 1–7 fail on one or more of the following points:

- Precise synchronisation between dust dispersion and spark onset must be available.
- The energy losses must be insignificant or taken into account when calculating the spark energy.

- The sparks produced should be as similar as possible to purely capacitive electrostatic discharges.

The objective of the present work has been to develop a spark generation method that fulfils all three requirements.

2.2. Spark energy measurement

The minimum spark energy that can ignite gases or dust clouds is a central parameter in hazard evaluation. It is therefore essential to be able to precisely measure or estimate the energy delivered to the spark, taking into account energy losses in other circuit elements.

The simplest method for calculating spark energy is based on the capacitor energy formula, i.e. the difference between stored capacitor energy before and after the discharge:

$$E = \tfrac{1}{2}C(V_B^2 - V_A^2),$$

where C is the capacitance, V_B is the capacitor voltage before discharge and V_A is the voltage after discharge. Usually, $V_B \gg V_A$ and thus the energy can be approximated by

$$E = \tfrac{1}{2}CV_B^2. \quad (1)$$

Whether the spark energy can be accurately estimated by this simple expression depends on the characteristics of the discharge circuit. If the discharge circuit contains resistive elements in series with the spark, some of the energy is inevitably lost, and not delivered to the spark. Even so, the gross capacitor energy gives an estimate of the energy in conventional MIE tests for dust clouds [1,2]. At low energies, accurate determination of stray capacitances is essential for precise energy estimation. This must be taken into account when introducing additional circuit elements, e.g. voltmeters and switches. Energy losses due to corona discharge, series resistance and radiation are not taken into account in this approach to the energy measurement calculation.

When estimating the discharge purely based on stored capacitor energy, little information about the discharge characteristics, e.g. spark duration and waveforms, is obtained. When measurements of circuit variables are made, the energy can be calculated from the integral of the power, i.e. the product of voltage v and current i of the spark, over the duration of the discharge:

$$E = \int v\,i\,\mathrm{d}t. \quad (2)$$

Thus, only the energy delivered to the spark is found, and circuit capacitance and losses are implicit. A major challenge to this approach is the fact that the different spark phases (e.g. breakdown, arc and glow) have durations differing by orders of magnitude, and the currents and voltages are varying by orders of magnitude in the different phases.

The energy delivered to the spark may alternatively be estimated by subtracting the resistive losses from the stored capacitor energy [9]:

$$E = \frac{1}{2}CV_B^2 - \int R\,i^2\,\mathrm{d}t,$$

where R is the circuit resistance in series with the spark gap. Only the current flowing through the spark is measured, eliminating the need for voltage measurements.

Several workers in the field have reported spark energy measurements by calculation of voltage and/or current as functions of time. A review of the work prior to 1973 is given by Strid [5]. Newer work is reported by e.g. [6–8,10–23]. Measurements of only current in electrostatic discharges were made by Smallwood [24].

In general, few details on the measurements are reported in the literature. However, due to the transient nature of the discharge, attention should be drawn to the measurement technique used. This applies especially to low energies, where the measured signal may be of the same order as the superimposed noise signal. When high frequency measurements are made, parasitic capacitances and inductances in the circuit play an important role, and attention to these must be paid. More details on high frequency measurements are given by e.g. Smith [25].

3. Experimental

3.1. The discharge circuit

The present discharge circuit is able to produce synchronised capacitive sparks of low energy similar to the ones resulting from electrostatic discharges. The schematic layout is shown in Fig. 1.

The circuit can be considered in two steps; the generation of a high-voltage pulse, and the subsequent spark discharge of a capacitor charged by this pulse. By triggering a thyristor, a high-voltage pulse is generated by discharging a primary capacitor of 1 μF through a high-voltage transformer.[1] Discharge of the discharge capacitor occurs when the breakdown voltage is reached. Thus, synchronisation between dust dispersion and sparkover is possible.

By the use of a large charging resistor, the spark discharge is practically independent of the high-voltage pulse, because additional charging of the discharge capacitor is negligible within the lifetime of the spark. The resistance R of the charging resistor is chosen in

[1] A simple coil intended for spark ignition in automobile engines is used.

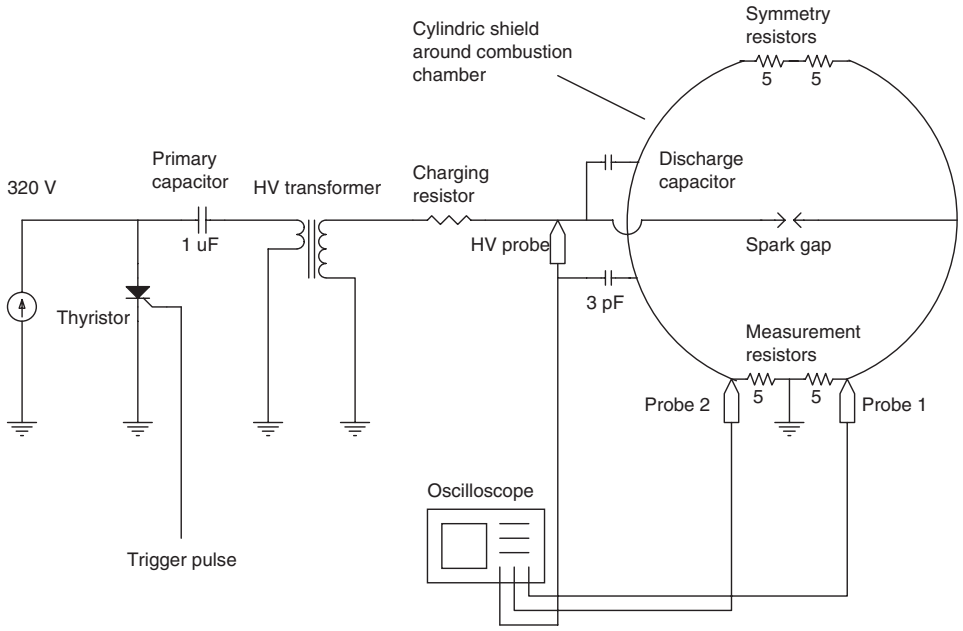

Fig. 1. Schematic layout of the discharge circuit and the measurement system.

such a manner that the time constant RC, where C is the discharge capacitance, is much larger than the duration of the discharge.

Typically, the charging resistance is between 100 kΩ and 1 MΩ, depending on the discharge capacitance. Thus, with a voltage drop of ~10 kV over the resistor, a current of no more than ~10 mA is recharging the capacitor. Because the current involved in a discharge of short duration (~100 ns) is much larger, only an insignificant amount of energy is added to the spark within its lifetime.

The capacitance values used in the present work are in the range of a few pF and about 250 pF. For the smallest capacitance values, primarily the stray capacitance between the electrodes contributes. Larger capacitance values are obtained by placing one or more parallel plate capacitors into the grounded electrode holder that constitutes the capacitor, shown in Fig. 2, with plates connected directly to the high-voltage electrode, separated by plastic from the electrode holder. The electrodes are sharpened (approximately 60° angle) 2 mm diameter tungsten rods, and the gap widths range from 1 to 6 mm in the work presented here. Photographs of the discharge circuit are shown in Fig. 3.

A system for voltage and current measurement is integrated in the circuit. Two measurement resistors are placed on each side of ground, and probes for balanced current measurements are placed over them. The measurement resistors are integrated in a cylindrical shield (diameter 11.5 cm) around the combustion chamber, and to ensure symmetrical current distribution identical resistors are integrated on the opposite side of the shield. A high-voltage probe is placed at the high-voltage electrode, and its capacitance of 3.0 pF must be taken into account when considering the capacitance involved in the discharge.

Only the capacitance behind the charging resistor contributes as energy storage for the spark, which means that the discharge can be considered as almost purely capacitive. The inductance of the circuit behind the charging resistor is only due to the geometric properties, and is of the order of 0.1 μH. The main difference between this circuit and other circuits used for triggered capacitive spark ignition (Section 2.1) is that no switches or other elements contribute with stray capacitances or inductances.

As long as the effect of the probes is taken into account, the circuit is very clear and simple to analyse. Thus, the arrangement yields a method of generating sparks quite similar to electrostatic sparks, without the use of a static high-voltage source. Because the high-voltage electrode is neutral except for a very short time before breakdown, corona losses can be neglected.

The discharge circuit has some similarities to the circuit presented in paragraph 2, Section 2.1, where a static high-voltage source is used to charge the capacitor instead of a high-voltage pulse. However, when a pulse is used, the time of spark discharge is much more precisely determined than when the discharge capacitor voltage is slowly raised until breakdown.

3.2. Spark energy measurement system

The spark energy measurement system is integrated in the spark generation circuit, shown in Figs. 1 and 3. The cylindrical shield surrounding the spark gap is

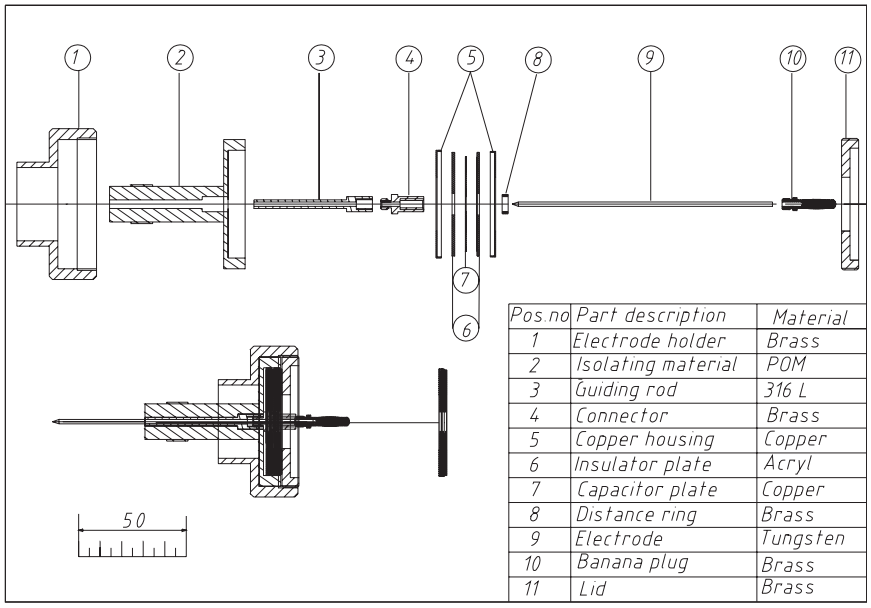

Pos no	Part description	Material
1	Electrode holder	Brass
2	Isolating material	POM
3	Guiding rod	316 L
4	Connector	Brass
5	Copper housing	Copper
6	Insulator plate	Acryl
7	Capacitor plate	Copper
8	Distance ring	Brass
9	Electrode	Tungsten
10	Banana plug	Brass
11	Lid	Brass

Fig. 2. Cross-section of the high-voltage electrode and the capacitor elements, showing how one or more parallel plate capacitors can be placed between the grounded electrode holder and the electrode.

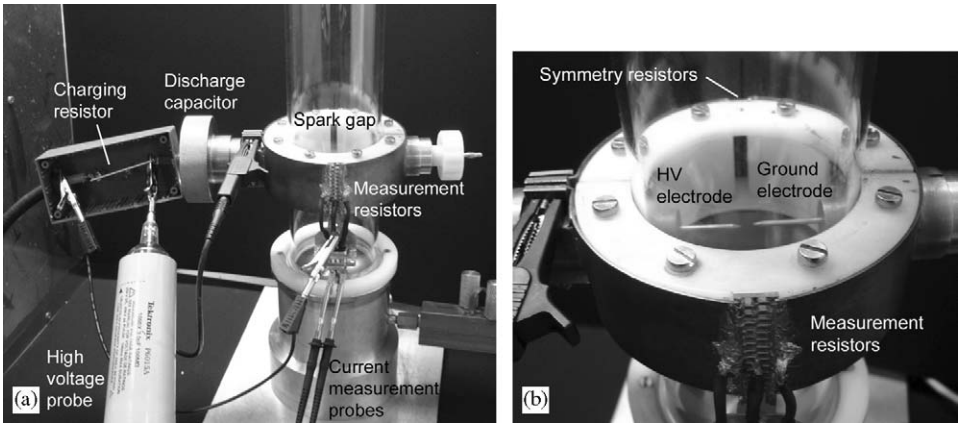

Fig. 3. (a) Discharge circuit and measurement system, showing the physical properties of the schematic circuit of Fig. 1. (b) The spark gap and measurement resistors in more detail.

motivated by the need to reduce the noise influencing the measuring probes.

Voltage measurements are made with a high-voltage probe (Tektronix P6015) placed at the high-voltage electrode and with its ground cable attached to the screen, as shown in the figures. The 3.0 pF probe capacitance thus adds to the discharge capacitance in parallel.

Several surface mounted resistors are mounted in parallel, with an overall resistance of 5 Ω, and are integrated in the shield. The voltage drops over two 5 Ω resistors give the spark current. Two separate current measurements are thus made, yielding the possibility to measure the spark current differentially. Conventional, passive scope probes (bandwidth 500 MHz) are used to measure the voltage drop. However, the standard ground loops (''pigtails'') are not used so that less noise is picked up.

Because of the symmetry resistors on the opposite side of the shield, the effective measurement resistance is 2.5 Ω on each probe. This value was chosen because of the amplitude of the signals generated for low-energy sparks. For capacitor energies higher than about 10 mJ, the signal may be too large to be handled by the oscilloscope. This can easily be overcome by reducing the resistor value.

The oscilloscope used for data acquisition is a Tektronix TDS 3034B, with a bandwidth of 300 MHz, a maximum sampling rate of 2.5 GS/s, four channels, 9-bit vertical resolution and 10,000 points horizontal resolution. Two channels are used for the current signals, and one for the voltage.

The stated bandwidth of the high-voltage probe is 75 MHz. In order to investigate how this affects the voltage measurements, a square pulse with very short rise time (generated by pulse generator Stanford Research Systems DG535) was measured with both the high-voltage probe and a scope probe simultaneously. The high-voltage probe was found to yield signals delayed by 9.0 ns compared to the scope probe, but with little distortion of the pulse shape. Therefore, only adjustment for the time delay was done when importing the oscilloscope traces into the computer.

The discharge energy was calculated in a spreadsheet, by integrating the product of voltage and balanced current in accordance with Eq. (2). The time scale was defined by setting the time $t = 0$ at first peak of the damped oscillating current trace. Energy integration was made between $t = -20$ and 100 ns, which assured sufficient duration to obtain the total energy. For calculations of the net spark energy E_S, the energy delivered to the current measurement resistors was subtracted according to the following expression:

$$E_S = \int v\, i\, dt - \int R_M\, i^2\, dt, \tag{3}$$

where R_M is the total resistance of the measurement resistors and the symmetry resistors, equal to 5 Ω.

The stored capacitor energy prior to discharge was calculated by measurement of the circuit capacitance and the voltage prior to breakdown, according to Eq. (1). The capacitance was measured with an *RCL* meter (Philips PM 6303) connected at the electrode tips. The voltage prior to breakdown was found from the high-voltage probe measurements.

3.3. Equivalent discharge circuit simulations

Based on the simple discharge circuit in the right-hand side of Fig. 1, an equivalent circuit can be made. Assuming no additional charging of the discharge capacitor takes place within the duration of the discharge, the input pulse can be considered a step pulse, which initiates breakdown at a capacitor voltage equal to the amplitude. The spark gap is replaced by a variable resistor R_S, which is assumed to be only a function of the energy delivered to the spark. The time-dependent spark resistance is chosen inversely proportional to the energy delivered to the spark. A schematic layout of the simulation model is shown in Fig. 4.

The following coupled differential equations, based on the mathematical relationship between voltage and current in circuit elements, describes the equivalent circuit:

$$V_{in} = \frac{1}{C}\int i\, dt + L\frac{di}{dt} + R_M i + R_S i.$$

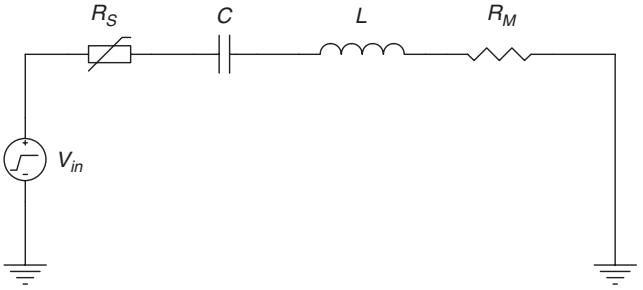

Fig. 4. Equivalent discharge circuit. The spark gap is replaced by a variable spark resistance R_S. C is the discharge capacitance, L the inductance and R_M the value of the measurement resistors. The input pulse V_{in} is a step pulse with amplitude corresponding to the breakdown voltage.

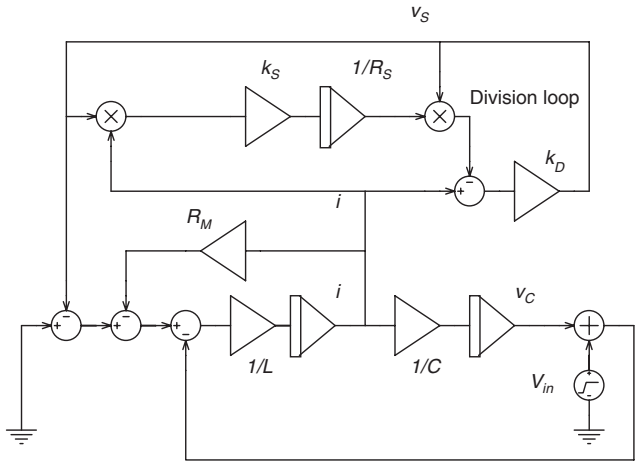

Fig. 5. Block diagram of the simulated discharge circuit of Fig. 4.

Because all of the circuit elements are in series, the current i flowing through the elements is common. The assumed relation between spark resistance and spark energy can be represented in the following way:

$$\frac{1}{R_S} = k_S E_S = k_S \int v_S\, i\, dt, \tag{4}$$

where k_S is an adjustable spark constant. A simulation was made in *Cadence PSpice*, using a block diagram instead of direct circuit simulation because of the variable resistor R_S. The block diagram is shown in Fig. 5, with constants illustrated by triangles, and integrations by triangles with a double vertical line. A realisation of Eq. (4) in the block diagram is made by numerical division of spark current and voltage by the use of a division loop. The following approximation is made to obtain an expression for the inverse spark resistance:

$$(i - k_S E_S v_S) k_D = v_S,$$

$$\frac{i}{v_S} \simeq k_S E_S,$$

where the division constant k_D is a very large number.[2] Known circuit parameters are used as input for the discharge capacitance C and the measurement resistors R_M. The proportionality factor k_S between the spark conductivity and energy can be tuned so that curves similar to the measured voltage and current curves are obtained. The circuit inductance, which is a function of the geometry of the circuit, is estimated from the oscillation frequency found in the current and voltage measurements. The resonance frequency is simply given by the formula for an LC circuit

$$f = \frac{1}{2\pi\sqrt{LC}}. \quad (5)$$

The capacitor voltage v_C and the circuit current i are equivalent to the parameters measured by the oscilloscope.

4. Results and discussion

4.1. Measured current and voltage waveforms and spark energies

Owing to the construction of the circuit, discharge current and voltage show quite "pure" capacitive discharge characteristics, i.e. the spark is scarcely prolonged due to added impedance. Discharge times are typically less than 80 ns, which is consistent with the measurements of electrostatic discharge current made by Smallwood [24]. The pulses are oscillatory, in accordance with the low circuit resistance of the discharge circuit [26].

Typical voltage and current curves are given in Figs. 6 and 7, and the corresponding cumulative energies are given in Fig. 8. The electrode gap is 4 mm, and the presented curves are chosen from ten trials at each configuration in such a way that some scattering of the curves could be obtained. This choice was made for purely illustrational purposes.

It is worth noting that the steepness of the voltage drop in Fig. 6 is depending on the circuit capacitance, which can be related to the time constant RC. Larger capacitors need longer time to discharge than smaller ones at a given circuit resistance. The breakdown voltage depends primarily on the electrode gap.

The current traces depend strongly on the discharge capacitance. This applies to both amplitude and pulse width, but the shapes of the current traces are quite similar. Both the voltage and current traces have the characteristics of damped oscillations. However, the oscillation frequency is depending on the capacitance, which is reasonable when treating the discharge circuit as an RLC-circuit. The inductance L is a function of the

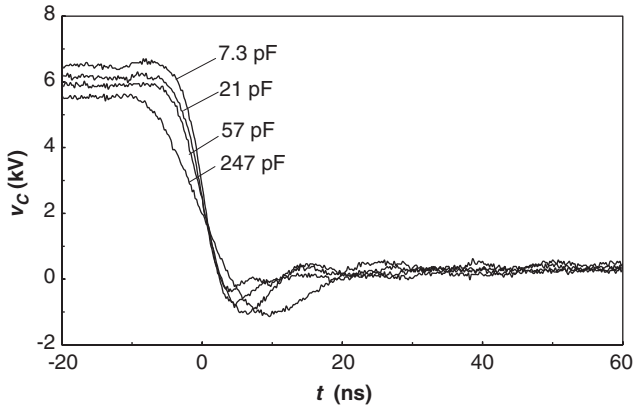

Fig. 6. Measured capacitor voltages v_C as a function of time for different capacitance values. The electrode gap is 4 mm.

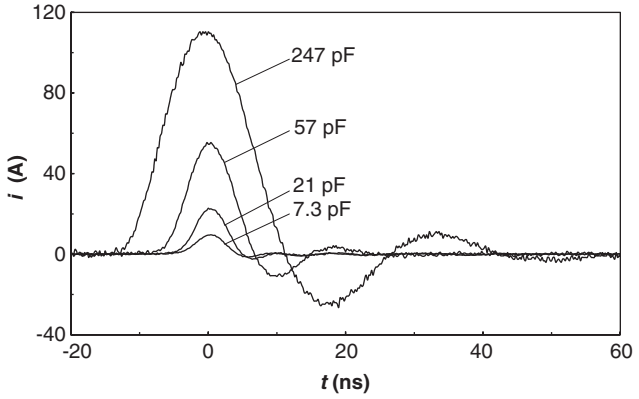

Fig. 7. Balanced current i as a function of time for different capacitance values. The current traces are from the same discharges as the corresponding voltage traces in Fig. 6.

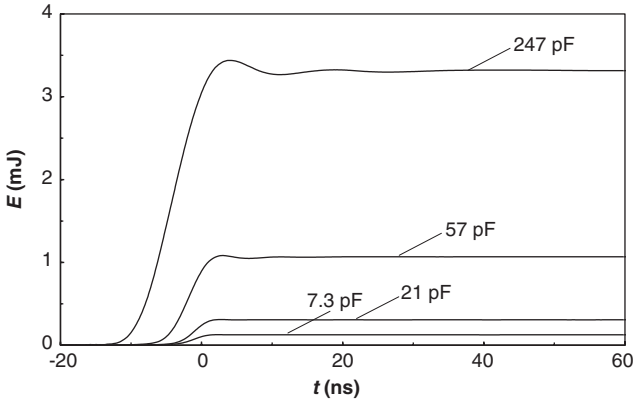

Fig. 8. Integrated discharge energy E for different capacitances. The energies are calculated from the voltage traces given in Fig. 6 and current traces in Fig. 7, applying Eq. (2).

[2]The error made with this approximation is very small, but is actually essential for making this simulation approach work. With an exact division, the spark conductivity is zero permanently, and no current will flow.

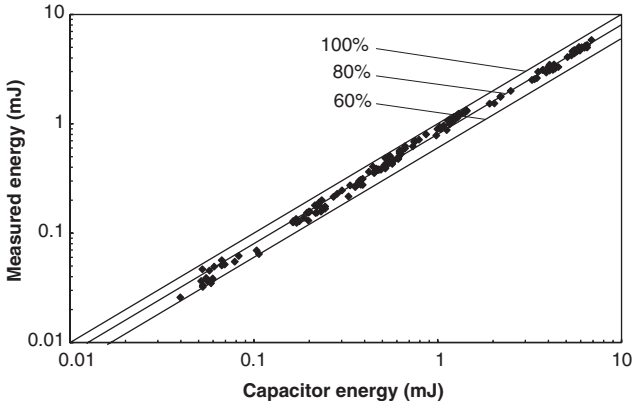

Fig. 9. Measured discharge energy plotted versus initially stored capacitor energy $\frac{1}{2}CV^2$. Ten measurements are made at four different capacitor values and four spark gaps. The straight lines correspond to 100, 80 and 60 per cent of the capacitor energy.

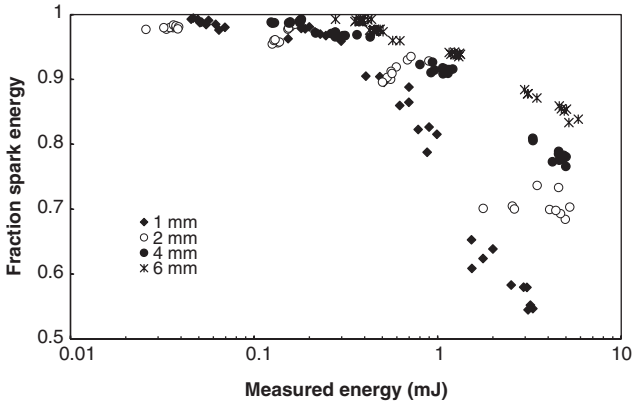

Fig. 10. Fraction of the total measured energy delivered to the spark as a function of measured energy for four different electrode gaps, calculated according to Eq. (3). Ten measurements are made at each capacitor value and spark gap.

geometrical properties of the circuit, being virtually constant for varying capacitors. The resonance frequency of the current traces of Fig. 7 is depending on C as given by Eq. (5). An increase in oscillation frequency when the capacitance is reduced is observed, indicating that the spark is mainly resistive.

The relation between measured discharge energy and stored discharge capacitor energy prior to breakdown ($\frac{1}{2}CV^2$) is shown in Fig. 9, where measured energy is plotted versus capacitor energy. Ten measurements are made for four different capacitor values and four spark gaps, with energies ranging between 0.03 and 7 mJ. The measured energy corresponds to between 60 and 90 per cent of the capacitor energy. The fraction of the energy lost in radiation, to the electrodes, because of skin effect resistance, and left on the capacitor is typically 20 per cent. However, the scattering may also be related to numerical errors, especially at the lowest voltages when inaccurate breakdown voltages have a relatively larger influence on the calculation of capacitor energy. In addition, inaccurate measurement of the lowest capacitances values may also be part of the explanation.

The net spark energy, calculated from the expression in Eq. (3), constitutes an increasingly bigger part of the total measured energy as the capacitance decreases, because the energy loss to the measurement resistors is only significant when a relatively large current is flowing through them. The fraction of the measured energy delivered to the spark is shown in Fig. 10. For energies above about 0.4 mJ, the losses to the measurement resistors become significant. The effect is increasingly pronounced at small electrode gaps, indicating that larger currents flow when the spark is short.

4.2. Circuit simulation results

Based on the oscillation frequency of the measured current curves, an inductance of 0.095 μH is used in the simulations, together with the actual circuit capacitance (including the high-voltage probe's capacitance), the 5 Ω measurement resistor and the breakdown voltage.

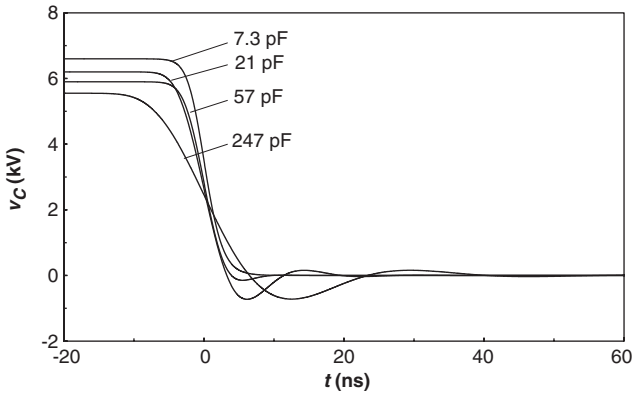

Fig. 11. Simulated capacitor voltage traces resulting from the equivalent discharge circuit of Fig. 4. The spark constant k_S is tuned in order to acquire similarity to the measured curves of Fig. 6.

The spark constant k_S was adjusted in each trial until the simulated voltage and current matched its measured counterparts. The simulated capacitor voltages for different capacitance values are shown in Fig. 11, corresponding to the measured voltages of Fig. 6, and equivalent for the simulated currents in Fig. 12 and the measured currents of Fig. 7.

The behaviour of the simulated and measured curves was quite similar, but some discrepancies were found. The oscillation frequencies are not in complete agreement at all capacitances, indicating that the spark has a certain inductive component. In addition, the simulated curves tend to be more damped than the measured ones, also indicating that the simple assumption of pure resistive spark behaviour is somewhat inaccurate.

The spark constant k_S is plotted versus the input voltage of the step pulse, corresponding to the breakdown

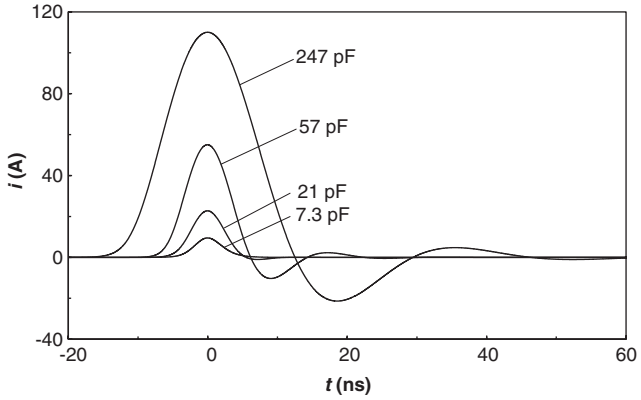

Fig. 12. Simulated current traces corresponding to the voltage traces of Fig. 11.

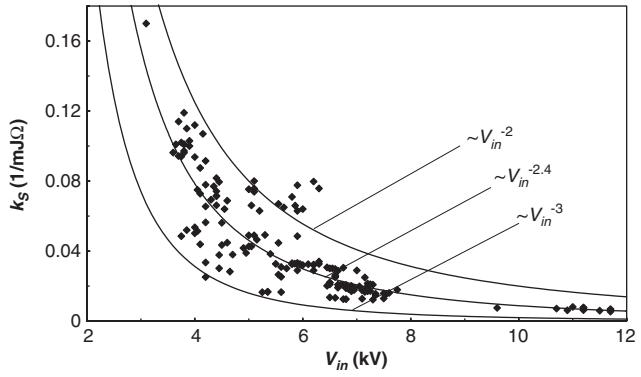

Fig. 13. Spark constants k_S plotted versus input pulse voltages V_{in}, corresponding to the measured breakdown voltages. The middle curve is the result of a regression analysis assuming a power-law correlation.

voltage, in Fig. 13. By regression, the following correlation was obtained:

$$k_S = 2V_{in}^{-2.4}\left[\frac{1}{mJ\Omega}\right],$$

where the input voltage is given in kilovolts. Two additional curves are added in the figure, with exponents of -2 and -3, respectively. Significant deviation from the correlation curve indicates that the assumption of a pure resistive spark, only depending on the spark energy, is too simple. However, reasonable agreement between the measured and simulated results has been achieved using this simple assumption, and the spark constant clearly depends on the breakdown voltage.

5. Conclusions

1. A new electrical circuit for generation of low-energy electric sparks, from capacitive discharges, has been developed and investigated. The method of spark triggering provides a means for producing synchronised sparks for MIE determination for dust clouds in the energy region below the lower limit of a few mJ in current standard tests. The sparks generated from the new circuit are similar to the ones resulting from accidental electrostatic spark discharges in industrial practice. The energies of the investigated discharges are between 0.03 and 7 mJ.
2. A measurement system for capturing voltage and current waveforms has been included in the spark generation circuit, giving the opportunity to acquire the energy delivered to the spark by integration of the power-time trace. The measurement system's influence on the discharges, and methods of noise reduction, are important for producing reliable results. The durations of the discharges generated by the new circuit are quite short—less than 100 ns—indicating that the breakdown phase is dominating.
3. By integration of the power, the spark energies were measured to constitute between 60 and 90 per cent of the energy stored on the capacitor prior to breakdown ($\frac{1}{2}CV^2$). Losses in the measurement resistors are increasingly significant at high energies and large electrode gaps.
4. A simple simulation, assuming a time-dependent spark conductivity proportional to the spark energy, yields currents and voltages in reasonable agreement with the measured results. The discharge channel's ability to carry current is strongly depending on the energy supplied, and the spark is mainly resistive. The proportionality factor is found to depend on the breakdown voltage.

Acknowledgements

This work was supported financially by the Research Council of Norway. The authors would like to thank GexCon AS for lending some of the equipment used.

References

[1] CEN, Determination of Minimum Ignition Energy of Dust/Air Mixtures, European Standard EN 13821, European Committee for Standardization, Brussels, 2002.
[2] IEC, Method for Determining Minimum Ignition Energies of Dust/Air Mixtures, IEC International Standard 1241-2-3, International Electrotechnical Commission, Geneva, 1994.
[3] B. Lewis, G. von Elbe, in: B. Lewis, G. von Elbe (Eds.), Combustion, Flames and Explosions of Gases, third ed, Academic Press, London, 1987.
[4] W. Bartknecht, Explosionsschutz, Springer, Berlin, 1993.
[5] K.-G. Strid, Experimental techniques for the determination of ignition energy, Oxid. Combust. Rev 6 (1973) 1–46.
[6] S.J. Parker, Electric spark ignition of gases and dusts, Ph.D. Thesis, The City University, London, 1985.
[7] D.R. Ballal, A.H. Lefebvre, The influence of spark discharge characteristics on minimum ignition energy in flowing gases, Combust. Flame 24 (1975) 99–108.

[8] D.R. Ballal, A.H. Lefebvre, Ignition and flame quenching in flowing gaseous mixtures, Proc. R. Soc. Lond. A 357 (1977) 163–181.
[9] H.G. Riddlestone, The effect of series resistance on the energy dissipated in capacitive spark discharges across small gaps, ERA Report G/T253, The British Electrical and Allied Industries Research Association, 1951.
[10] B. Alvestad, An Electric Spark Generator for Determination of Minimum Ignition Energies of Dust Clouds, CMI, Bergen, 1975 CMI Report No. 72001-12.
[11] R.K. Eckhoff, Towards absolute minimum ignition energies for dust clouds?, Combust. Flame 24 (1975) 53–64.
[12] M. Kono, S. Kumagai, T. Sakai, The optimum condition for ignition of gases by composite sparks, in: Proceedings of the 16th Symposium (International) on Combustion: The Combustion Institute, 1976, pp. 757–766.
[13] I.G. Buckland, An apparatus and method for determining the minimum ignition energy of dusts, Note N 24/79, Department of the Environment, Building Research Establishment, Hertfordshire, 1979.
[14] G.F.M. van Laar, Determination of the minimum ignition energy (MIE). Gross and net spark energy in the TNO spark circuit, G9548-G0093, Prins Maurits Laboratorium, Institute of Chemical and Technological Research, Rijswijk, The Netherlands, 1981.
[15] R. Maly, Ignition model for spark discharges and the early phase of flame front growth, in: Proceedings of the 18th Symposium (International) on Combustion: The Combustion Institute, 1981, pp. 1747–1754.
[16] R.S. Lee, et al., Improved diagnostics for determination of minimum explosive concentration, ignition energy and ignition temperature of dusts, Powder Technol. 31 (1982) 51–62.
[17] T. Matsuda, M. Naito, Effects of a spark discharge duration on ignition energy for dust–air suspension, in: J.K. Beddow (Ed.), Particulate Systems. Technology and Fundamentals, McGraw-Hill International Book Company, 1983, pp. 189–198.
[18] G.F.W. Ziegler, E.P. Wagner, R.R. Maly, Ignition of lean methane–air mixtures by high pressure glow and arc discharges, in: Proceedings of the 20th Symposium (International) on Combustion: The Combustion Institute, 1984, pp. 1817–1824.
[19] A. Norberg, N. Szedenik, S. Lundquist, On the pulse shape of discharge currents, J. Electrostat. 23 (1989) 79–88.
[20] J.M. Smallwood, A.G. Bailey, Low energy spark ignition of sensitive materials using pulse techniques, in: Proceedings of the 14th International Pyrotechnic Seminar, 1989, pp. 371–380.
[21] T. Matsuda, M. Yamaguma, Tantalum dust deflagration in a bag filter dust-collecting device, J. Hazard. Mater. 77 (2000) 33–42.
[22] U. von Pidoll, E. Brzostek, H.-R. Froechtenigt, Determining the incendivity of electrostatic discharges without explosive gas mixtures, IEEE Trans. Ind. Appl. 40 (2004) 1467–1475.
[23] K.S. Choi, et al., Effects of corona charging of coating polymer powders on their minimum ignition energies, J. Loss Prevent. Proc. 17 (2004) 59–63.
[24] J.M. Smallwood, Simple passive transmission line probes for electrostatic discharge measurements, Inst. Phys. Conf. Ser. (163) (1999) 363–366.
[25] D.C. Smith, High Frequency Measurements and Noise in Electronic Circuits, AT&T, New York, 1993.
[26] J.M. Smallwood, A.G. Bailey, Electrical discharge incendivity to a pyrotechnic powder, in: Proceedings of the 18th International Pyrotechnics Seminar, 1992, pp. 867–878.